

The Role of Numerical Simulation in the Design of Stimulation and Circulation Experiments for the EGS Collab Project

Mark White¹, Pengcheng Fu², Hai Huang³, Ahmad Ghassemi⁴, and EGS COLLAB Team⁵

¹Pacific Northwest National Laboratory, Richland, WA, USA

²Lawrence Livermore National Laboratory, Livermore, CA, USA

³Idaho National Laboratory, Idaho Falls, ID, USA

⁴The University of Oklahoma, Norman, OK, USA

Keywords

Numerical Simulation, EGS Collab, EGS, Sanford Underground Research Facility, Meso-Scale Experimental Design, Stimulation, Circulation, Hydraulic Fracture, Borehole Orientation, Borehole Notching, THMC Modeling

ABSTRACT

The United States Department of Energy, Geothermal Technologies Office (GTO) is funding a collaborative investigation of enhanced geothermal systems (EGS) processes at the meso-scale. This study, referred to as the EGS Collab project, is a unique opportunity for scientists and engineers to investigate the creation of fracture networks and circulation of fluids across those networks under in-situ stress conditions. The EGS Collab project is envisioned to comprise three experiments and the site for the first experiment is on the 4850 Level in phyllite of the Precambrian Poorman formation, at the Sanford Underground Research Facility, located at the former Homestake Gold Mine, in Lead, South Dakota. Principal objectives of the project are to develop a number of intermediate-scale field sites and to conduct well-controlled in situ experiments focused on rock fracture behavior and permeability enhancement. Data generated

⁵ T. Kneafsey, D. Blankenship, J. Ajo-Franklin, S.J. Bauer, T. Baumgartner, A. Bonneville, L. Boyd, S.T. Brown, J.A. Burghardt, S.A. Carroll, T. Chen, C. Condon, P.J. Cook, P.F. Dobson, T. Doe, C.A. Doughty, D. Elsworth, L.P. Frash, Z. Frone, P. Fu, A. Ghassemi, H. Gudmundsdottir, Y. Guglielmi, G. Guthrie, B. Haimson, J. Heise, C.G. Herrick, M. Horn, R.N. Horne, M. Hu, H. Huang, L. Huang, T.C. Johnson, B. Johnston, S. Karra, K. Kim, D.K. King, H. Knox, D. Kumar, M. Lee, K. Li, M. Maceira, N. Makedonska, C. Marone, E. Mattson, M.W. McClure, J. McLennan, T. McLing, R.J. Mellors, E. Metcalfe, J. Miskimins, J.P. Morris, S. Nakagawa, G. Neupane, G. Newman, A. Nieto, C.M. Oldenburg, R. Pawar, P. Petrov, B. Pietzyk, R. Podgorney, Y. Polsky, S. Porse, B. Roggenthen, J. Rutqvist, H. Santos-Villalobos, P. Schwering, V. Sesetty, A. Singh, M.M. Smith, N. Snyder, H. Sone, E.L. Sonnenthal, N. Spycher, C.E. Strickland, J. Su, A. Suzuki, C. Ulrich, N. Uzunlar, C.A. Valladao, W. Vandermeer, D. Vardiman, V.R. Vermeul, J.L. Wagoner, H.F. Wang, J. Weers, J. White, M.D. White, P. Winterfeld, Y.S. Wu, Y. Wu, Y. Zhang, Y.Q. Zhang, J. Zhou, Q. Zhou, and M.D. Zoback

during these experiments will be compared against predictions of a suite of computer codes specifically designed to solve problems involving coupled thermal, hydrological, geomechanical, and geochemical processes. Comparisons between experimental and numerical simulation results will provide code developers with direction for improvements and verification of process models, build confidence in the suite of available numerical tools, and ultimately identify critical future development needs for the geothermal modeling community. Moreover, conducting thorough comparisons of models, modelling approaches, measurement approaches and measured data, via the EGS Collab project, will serve to identify techniques that are most likely to succeed at the Frontier Observatory for Research in Geothermal Energy (FORGE), the GTO's flagship EGS research effort. As noted, outcomes from the EGS Collab project experiments will serve as benchmarks for computer code verification, but numerical simulation additionally plays an essential role in designing these meso-scale experiments. This paper describes specific calculations and numerical simulation approaches conducted in support of the designs for the stimulation and circulation experiments, and their monitoring, including those for predicting seismic energies during stimulation, stimulation pressure requirements, impacts of borehole orientation on fracture development and trajectories, influence of notch shapes on hydraulic fracture initiation, and pressure limits on fluid circulation to avoid fracture growth.

1. Introduction

In October 2016, the United States Department of Energy (DOE), Geothermal Technologies Office (GTO) announced a funding opportunity that was to be collaborative in nature and act as a research and development bridge between laboratory-scale stimulation and rock mechanics studies and the large field scale of the future Frontier Observatory for Research in Geothermal Energy (FORGE) investigations (U.S. Department of Energy, 2017). The recipient of the Collab award was announced in early 2017, the Stimulation Investigations for Geothermal Modeling Analysis and Validation (EGS COLLAB) project, lead by the Lawrence Berkeley National Laboratory (LBNL). This collaborative project involves national laboratories, universities and private industry teaming to conduct stimulation and circulation experiments, and verify computer codes, numerical algorithms and approaches, and process models against the generated data. This three-year project has been tasked with providing new knowledge and modeling capabilities, forming a bridge from laboratory scale to the field scale of FORGE.

Code verification is a critical element in the advancement of numerical simulators for enhanced geothermal systems (EGSs). DOE has supported the development and verification of numerical simulators throughout the history of EGS research, starting with the Finite Element Heat and Mass (FEHM), HDR Heat, and GEOCRACK models (Duchane and Winchester, 1993; Zvoloski, 2007), used to estimate the potential thermal lifetime of the Phase II Reservoir at Fenton Hill. More recently GTO sponsored a multiple-year code comparison study that considered nine benchmark problems and two challenge problems (White *et al.*, 2017; White *et al.*, 2016). The benchmark problems were structured to test the ability of the collection of numerical simulators to solve various combinations of coupled thermal, hydrologic, geomechanical, and geochemical processes. This class of problems was strictly defined in terms of properties, driving forces, initial conditions, and boundary conditions.

The challenge problems were based on the enhanced geothermal systems research conducted in hot dry rock at Fenton Hill, near Los Alamos, New Mexico, between 1974 and 1995. The Fenton

Hill Hot Dry Rock (HDR) project involved the stimulation, completion, and circulation testing in two separate reservoirs, distinguished by depth and flow complexity. Both challenge problems have specific questions to be answered via numerical simulation in three topical areas: 1) reservoir creation/stimulation, 2) reactive and passive transport, and 3) thermal recovery. Whereas the benchmark class of problems were designed to test capabilities for modeling coupled processes under strictly specified conditions, the stated objective for the challenge class of problems was to demonstrate what new understanding of the Fenton Hill experiments could be realized via the application of modern numerical simulation tools by recognized expert practitioners. Critical observations and data from the Fenton Hill experiments were varied and scattered among a number of individual experiments, and numerical simulation solutions were sought that satisfied as many observations as possible. Achieving agreement in multiple experimental observations from Fenton Hill often required participants to critically think about stimulation mechanisms involving natural and hydraulic fractures and re-evaluate their conceptual models and numerical solution approaches. This process has yielded new insights to Fenton Hill reservoirs and direction for future EGS research.

The EGS Collab project is a recognition of the importance of validating numerical simulation tools for EGS, and the meso-scale of the experiments and accessibility of the generated fracture networks under *in-situ* stress conditions and crystalline rock formations, and provides a unique opportunity for the validation of THMC modeling approaches. The EGS Collab project comprises three major experiments, occurring over the course of the three-year project duration. Each major experiment is composed of a series of smaller stimulation and circulation experiments. Prior to each experiment site characterization will be conducted and numerical simulations will be executed to guide the experimental design and monitoring systems. After each experiment, numerical simulations will be executed and results compared against the collected data. The diversity of the EGS Collab teams brings a spectrum of numerical approaches for modeling THMC processes for EGS (White *et al.*, 2016). The post experimental period will allow for comparison of these numerical approaches and an assessment of code limitations, need improvements, or alterations to conceptual models.

At this writing a site near the KISMET site (Oldenburg *et al.*, 2016), on the 4850 Level, has been selected for the first major experiment. This experiment involves two stages: 1) stimulation - the creation of a hydraulic fracture from a notched sub-horizontal borehole drilled nominally in the direction of the principal minimum horizontal stress (i.e., σ_h); and 2) circulation – the circulation of fluids between an injection well and one or more production wells intersecting the created fracture. Numerical simulations have been executed to address five specific questions concerning the design of these experiments:

1. What is the preferred stimulation borehole orientation to meet the project stimulation objectives?
2. Can a transverse hydraulic fracture form from the wellbore wall or is notching needed to promote propagation of transverse fractures?
3. How does notch geometry impact stimulation pressure and near wellbore impedance?
4. What are the anticipated number and magnitude of seismic events associated with the hydraulic stimulation?
5. What is the required duration for a chilled circulation experiment conducted at pressures that avoid fracture propagation?

This paper describes for each design question, the numerical simulation, modeling approach, and computer code applied to quantitatively answer the question, providing examples of the role of numerical simulation in EGS design and application.

2. Seismic Events and Magnitudes

A requirement for conducting work underground at SURF is an approved experimental plan and an element of that plan is an estimation of potential micro-seismicity resulting from the hydrofracture experiments. The question of what the anticipated number and magnitude of seismic events associated with the hydraulic stimulation was answered with numerical simulations executed with a fully coupled three-dimensional network flow and quasi-static discrete element model (DEM) (Zhou et al., 2017). The quasi-static DEM model, which is constructed by Delaunay tessellation of the rock volume, considers small-scale rock-fabric heterogeneities by using the “disordered” DEM mesh and adding random perturbations to the stiffness and tensile/shear strengths of individual DEM elements and the elastic beams between them. A conjugate 3D flow network based on the DEM lattice is constructed to calculate the fluid flow in both the fracture and porous matrix. One distinctive advantage of the model is that fracturing is naturally described by the breakage of elastic beams between DEM elements without complex and empirical ad hoc assumptions about fracture initiation and propagation direction. It is also extremely convenient to introduce mechanical anisotropy into the model by simply assigning orientation-dependent tensile/shear strengths to the elastic beams.

A detailed description of this numerical simulator is provided in Zhou et al. (2017), but a synopsis of the computational approach will be described here. The simulation consists of interleaved fluid flow, mechanical relaxation of the DEM network, recalculation of fracture permeability and beam breaking steps. The modeling of a hydraulic stimulation event starts with the calculation of new fluid pressures at the new time (i.e., old time + time step). These single-phase flow calculations follow Darcy’s law, using a finite-volume discretization with grid volumes centered on the conjugate flow node, and with the intrinsic permeability being dependent on the spacing being DEM particles that have been cleaved (i.e., had a connecting elastic beam break). Updated fluid pressures then act as forces on neighboring DEM particles, and the DEM network is relaxed to a new mechanical equilibrium by allowing the DEM particles to be displaced and rotated. DEM particle displacements and rotations yield changes of stresses in the connecting beams. If a beam connecting two DEM particles exceeds its failure criterion, then the beam is assumed to have broken, and is irreversibly removed from the DEM network. As particle displacements/rotations and beam failures are sequential events, the mechanical equilibrium computation is iterative, until no further beam breaking occurs, which concludes a time step.

One important concern that was raised by the physics experimental groups at SURF was how large the micro-seismicity would be from the hydraulic fracturing at KISMET. The DEM model calculates the elastic strain energy released from the broken beams during simulated fracturing events. Assuming each beam breakage is a single seismic event, and further assuming all elastic strain energy stored in the beams prior to breaking is used in generating seismicity, the DEM model then provides an estimate of the potential seismic magnitude. Heterogeneity was included in these numerical simulations by using a disordered DEM mesh and random perturbations in the equivalent geomechanical properties of the rock by altering the tensile and shear strengths of the

individual DEM elements and connecting elastic beams. These heterogeneities yield variations in the tensile stress concentrations at the outer fracture perimeter, producing a growth front with episodic bursts of expansion (i.e., micro-seismic events). The simulation was executed on a 15.24 m x 15.24 m x 9.14 m domain, using a total of 118,634 DEM particles, with water injection occurring in the middle of the domain over a 0.91-m vertical interval at a rate of 2 L/min. The simulation time was 345 s, with 0.5 s time steps.

Fluid pressure in the wellbore, exhibited the classical sharp increase to a breakdown pressure, followed with a sharp decrease to a propagation pressure, which decayed with increase in the fracture radius. The simulation is initialized by imposing the *in-situ* stresses as strain energy in the elastic beams connecting the DEM particles. As the beams break with fluid injection, this strain energy is released. Estimates of the magnitude of the seismic events that occurred during the stimulation were developed by considering each beam break as an event, or by summing the released energy over a time step. The latter approach yields a maximum during the initial fracture opening state of about 37.5 kJ, which is equivalent to a 0.1 magnitude on the Richter scale. Spatial-temporal distributions of seismic events and magnitudes are shown in Figure 1(a). In general, most of the simulated events are relatively small. Simulated energy release versus time is shown in Figure 1(b), where individual events during each time step were grouped into a single equivalent event. The largest energy release happened at the initial fracture opening stage, which has the most beam breakage events. After the initial opening, the fracture propagates smoothly (on average) under constant rate injection, with a few relatively large events (spikes shown in Figure 1(b)).

3. Borehole Orientation

Current estimates of the *in-situ* stress state at the first experiment site on the 4850 Level at SURF are $\sigma_v = 41.8$ MPa (Oldenburg et al, 2016), $\sigma_h = 21.7$ MPa, with a 356° trend and 12° plunge indicating fractures that are striking N 86° E with a dip of 78° to the southeast (Oldenburg et al, 2016), and $\sigma_H = 33.4 - 37.6$ MPa. The kISMET stimulation borehole was drilled nearly vertical and the near vertical fracture that resulted from hydraulic stimulation had a surface normal generally oriented toward the direction of σ_h , with little influence in orientation on rock fabric. Boreholes for the first EGS COLLAB experiment will be drilled from the West Access Drift, near the kISMET site. The drift in this region of SURF is both wider and taller than normal, allowing the drilling of HQ sized boreholes (diameter = 96 mm) in any orientation. The central project objectives for the first experiment are to stimulate a fracture with a diameter of approximately 10 m, and then circulate fluid through the fracture via injection and production wells, both hydraulically connected to the generated fracture. The highest probability of a borehole, other than the stimulation borehole, being hydraulically connected to a fracture would be one drilled in the direction of σ_h , orthogonal to the fracture plane. The question of borehole orientation, therefore, is most applicable to the stimulation well. To answer this question a series of numerical simulations were conducted by three teams that modeled fracture initiation and propagation from different stimulation borehole orientations, with respect to the principal stress directions and magnitudes.

The team from The University of Oklahoma (OU) applied their GeoFrac2D model to study possible fracture trace angles at the wellbore, and utilized the GeoFrac3D computer code for two borehole orientations; vertical and horizontal in the direction of σ_h . For the later orientation three

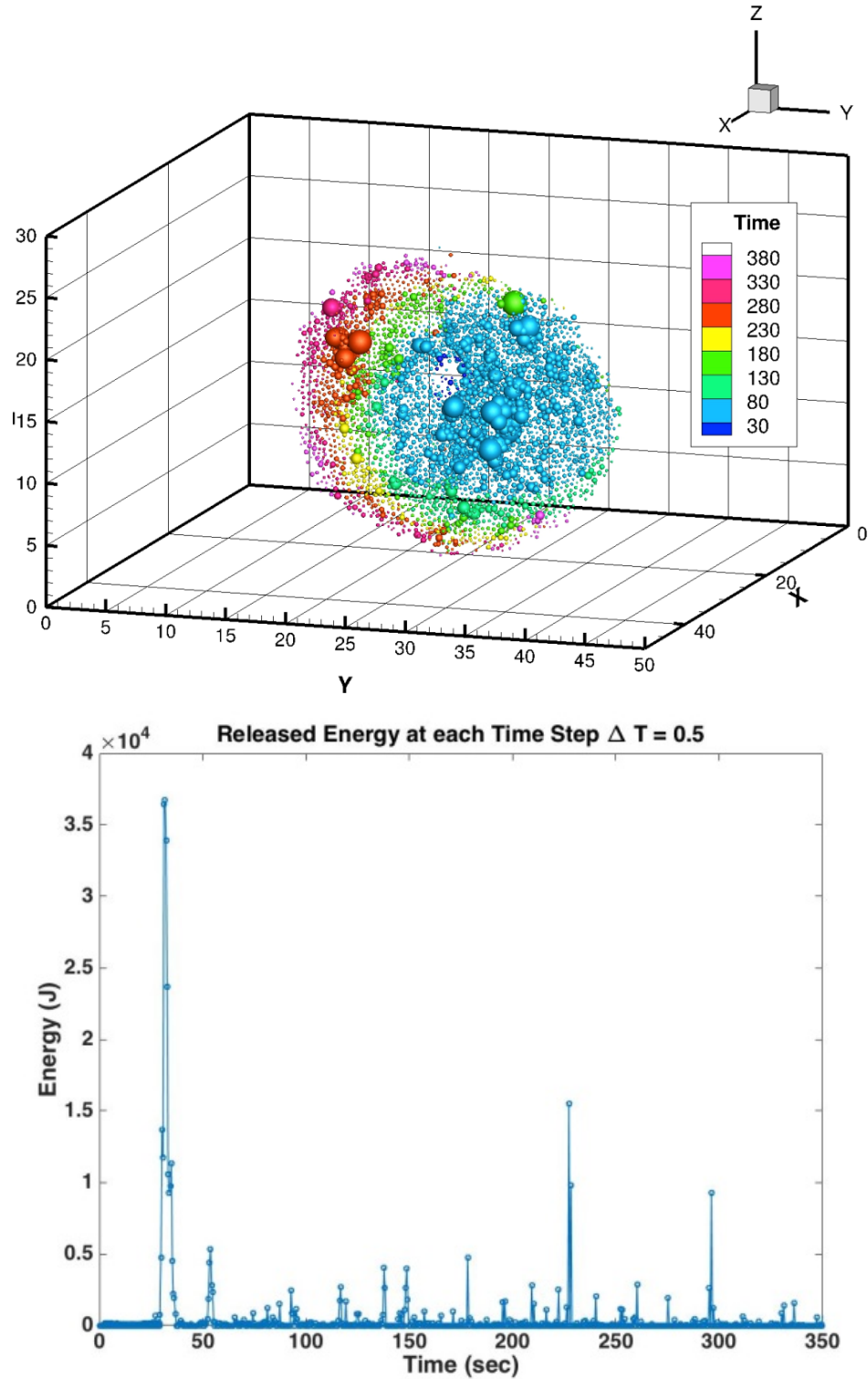


Figure 1: (a) Seismic events generated by the coupled network flow-DEM model. The color of each sphere represents time and the size of sphere is proportional to event magnitude, (b) released energy vs. injection time.

fracture initiations were considered, 90° (transverse), 30° , and 0° (longitudinal) inclination to the direction of the borehole. The 2D simulations showed that it is not possible to initiate a transverse fracture at the wellbore and that likely a longitudinal fracture would form suggesting that some type of notching is needed.

In this application GeoFrac3D's boundary element model solved the fracture mechanics component of the problem and its finite element model solved the single-phase fluid flow component. As the vertical borehole orientation was essentially equivalent to the kISMET configuration, the kISMET experiment was used to calibrate key parameters. An initial fracture radius of 0.2 m was assumed oriented 5.3° from the borehole axis, which was deviated 5° (based on fracture trace analysis considering rock anisotropy) from vertical. The six water injection cycles were simulated and good agreement was achieved between the experimental and simulation results in terms of borehole pressure and fracture radius versus time. Fracture propagation rotated during the first injection cycle in response to the principal stress directions as shown in Figure 2. Simulations of horizontal orientations ignored wellbore stress and produced expected results for borehole pressures versus fracture propagation and rotation of the fracture in response to the principal stresses for the fractures initially inclined 30° and 0° . Simulation results further demonstrated the influence on fracture turning radius with fluid injection rate (i.e., higher injection rates yielding longer turning radii).

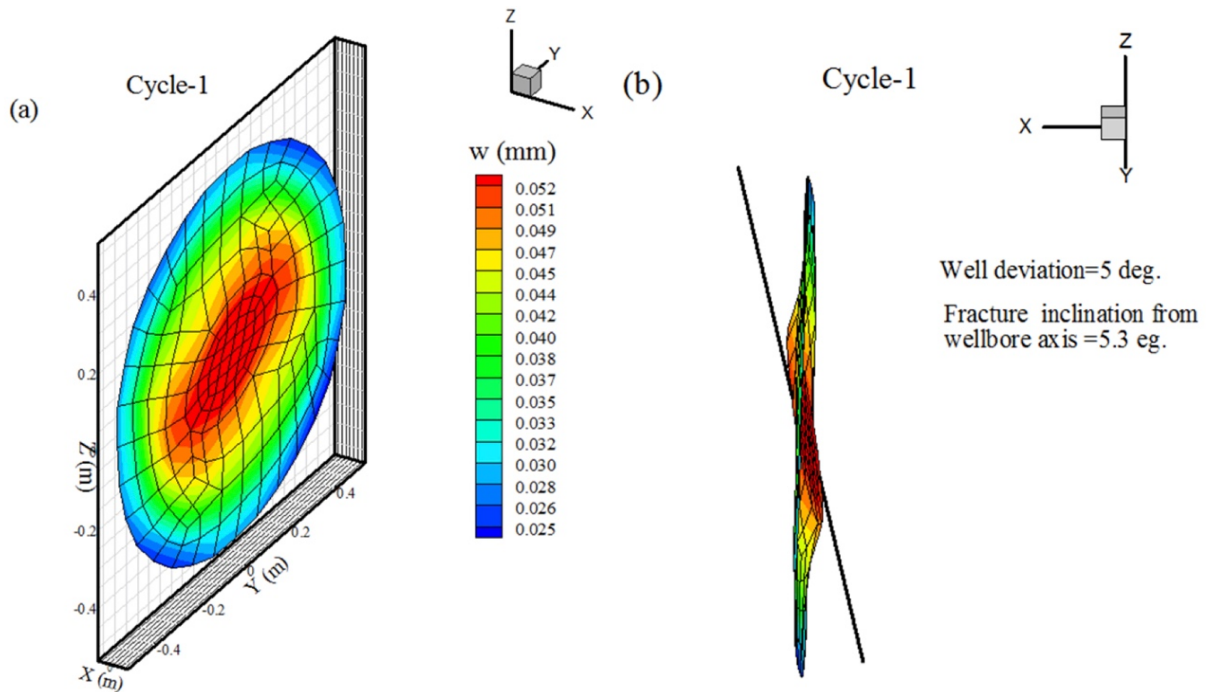


Figure 2: Fracture propagation during first injection cycle at kISMET (a) aperture and (b) orientation.

The team from Idaho National Laboratory applied the finite-element geomechanics capabilities of the FALCON (Fracturing And Liquid CONvection) (Gaston *et al.* 2012a,b; Podgorney *et al.* 2010) code to investigate under which *in-situ* stress and injection pressure conditions would preferentially yield initially axial or transversely oriented fractures from a horizontal borehole,

drilled in the direction of σ_h . For this investigation, the borehole was assumed to be smooth walled, without defects, and the mechanical properties of the host formation were homogenous. During the first sequence of simulations uncertainty in σ_H was addressed, by holding $\sigma_v = 42$ MPa, $\sigma_h = 21$ MPa, and the injection pressure = 80 MPa, and varying σ_H around that for σ_v . For these scenarios, an initially axial oriented fracture was possible for $\sigma_H = 32$ MPa. During the second sequence of simulations the impact of injection pressure was considered for constant *in-situ* stress conditions (i.e., $\sigma_v = 42$ MPa, $\sigma_h = 21$ MPa, $\sigma_H = 42$ MPa). For injection pressures from 25 to 80 MPa, no hoop or axial stresses around the borehole were computed to be tensile, indicating fracture initiation was unlikely. A third sequence of simulations were conducted at $\sigma_H = 22$ MPa at various injection pressures. These simulations indicated tensile hoop stresses at injection pressures above 35 MPa, indicating the likeliness of an initially axial oriented fracture. The principal outcome from this work was that for a horizontal or sub-horizontal borehole oriented in the direction of σ_h , and σ_H close in value to σ_v , as anticipated for the site of the first experiment, that notching the borehole would reduce the fracture initiation pressure and yield a fracture preferentially oriented in the transverse direction to the borehole.

4. Borehole Notching

After the EGS COLLAB team reached a consensus that a horizontal (or sub-horizontal) borehole along the σ_h direction would provide a desired relative orientation between the wells and the fracture, thereby reducing near-well pressure loss during circulation, the focus of the LLNL team's investigation turned to optimizing the design of wellbore notching that generates stress concentration. Such stress concentration is necessary for initiating a hydraulic fracture perpendicular to the wellbore direction because pressurization of a smooth wellbore, cylindrical in shape, has very little effects on the axial stress along the wellbore, according to Kirsch's equations. Various notching mechanisms had been considered, including abrasive perforation, shape charges, and mechanical notching. Due to the desire to avoid explosives and logistic complexities, mechanical notching is being considered as a favorable solution. The objective of the study documented in the current section is to quantify the effects of notch geometries on stress concentration near the notch when both the wellbore and the notch are subjected to fluid pressure.

Per discussion with designers of the perspective notching device at Sandia National Laboratories, we consider the geometry shown in Figure 3(a). We first assume a smooth semi-circular cross-section. Although the actual notch is likely to have sharp, irregular shapes, we analyze the smooth shape for the following considerations:

1. The smooth shape induces stress concentration but not stress singularity, allowing robust stress analysis less sensitive to mesh resolution and also permits direct comparison between different geometries.
2. The smooth shape represents the "worst-case scenario". If tensile stress can be generated by this shape, the stress caused by a rough surface with the same depth (H) and width (W) is likely to be more favorable for fracture initiation.
3. What the results reveal is essentially for a given notch front geometry (smooth or shape), how the notch depth and width affect the stress concentration.

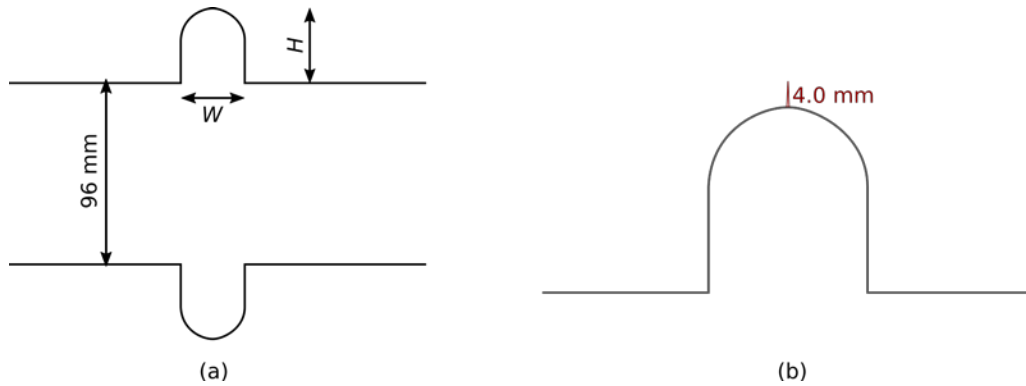


Figure 3: Notch geometry considered in this analysis. (a) A smooth notch surface for stress analysis with notch depth H and notch width W as variables. (b) Assuming a 4-mm deep crack at the crown of the smooth notch for fracture mechanics analysis. Illustration not to scale.

In addition to the stress analysis, we perform a parallel fracture mechanics analysis by introducing a small fracture, 4 mm deep, around the notch as shown in Figure 3 (b). The stress analysis and fracture mechanics analysis results should be interpreted in a unified, mutually complementary fashion. Having sufficient tensile stress (in comparison with tensile strength of the rock) at the crown of the notch would result in a small fracture like that depicted in Figure 3 (b), but this is not a sufficient condition for continued fracture growth as the generation of the small fracture could relax the stress concentration. Therefore, the role of the fracture mechanics analysis is to see if sufficient stress singularity (quantified by stress intensity factor in comparison with toughness of the rock) can be generated at the tip of the small fracture.

We assume the rock to be linearly elastic and isotropic. The packed-off wellbore is 0.8 m long and 96 mm in diameter. The simulation domain is a cylinder 4.8 m long and 4.0 m in diameter, sufficiently large (to represent the far field rock) compared with the wellbore geometry. Fluid pressure is applied on the surface of the wellbore, the two ends of the packed-off interval, the surface of the notch, and both walls of the 4-mm crack if applicable.

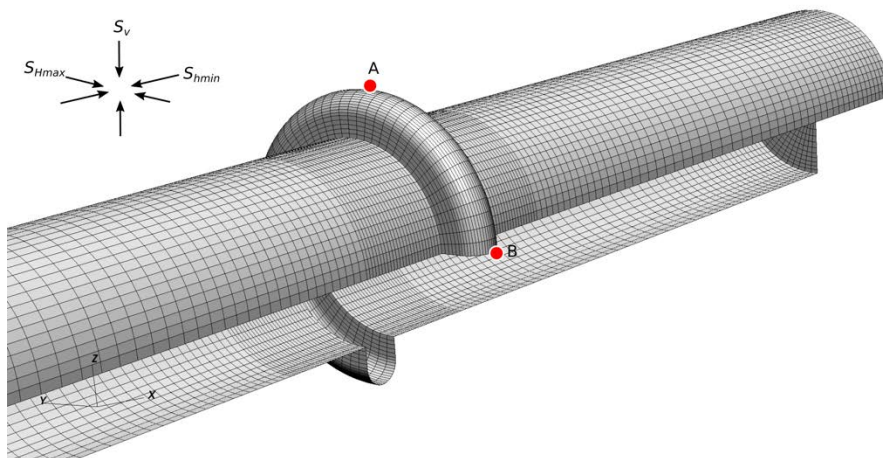


Figure 4: Mesh of the "skin" of the wellbore and the notch with $H = 20$ mm and $W = 20$ mm.

The mesh of the “skin” of the wellbore and the notch is shown in Figure 4. We establish a coordinate system with the x-axis along the σ_h direction, y-axis along σ_H and z-axis pointing upwards. The symmetry in the system dictates that the highest tensile stress should emerge at either point A (top) or point B (side). The mesh resolution near the notch is 1 to 2 mm and larger elements are used in the far-field. The whole model includes approximately 1.6 million elements. Material properties are based on the kISMET report with Young’s modulus of 71.4 GPa and Poisson’s ratio of 0.22.

Taking advantage of the linearity of the system, instead of analyzing the stress state under a specific set of assumed *in situ* stress and fluid pressure, we derive, through finite element analysis, the “transfer function” from individual stress/pressure components to the response of interest, e.g. σ_x^A or tensile stress at point A in the x-direction, namely

$$\sigma_x^A = T_h\sigma_h + T_H\sigma_H + T_V\sigma_V + T_P P \quad (1)$$

where T_h , T_H , T_V , and T_P are the four coefficients of the transfer function. Note that each coefficient is a function of the notch geometry. Once we obtain the values of these coefficients, we can calculate the stress of interest for any combination of in situ stress and wellbore pressure.

First we consider the tensile stress at point A (σ_x^A). We simulate nine geometries as summarized in Table 1 and obtain the transfer function coefficients. Note that due to symmetry, the coefficients for point B are identical to those for A except that T_H and T_V are swapped.

Table 1 Coefficients for the transfer function for tensile stress at point A. The last column shows the stress value corresponding to $\sigma_h = 21.7$ MPa, $\sigma_H = 35.5$ MPa, $\sigma_V = 41.8$ MPa, and $P = 35$ MPa.

| H (mm) | W (mm) | T_h | T_H | T_V | T_P | σ_x^A (MPa) |
|----------|----------|--------|--------|-------|-------|--------------------|
| 20 | 20 | -2.842 | -0.355 | 0.683 | 1.513 | 7.22 |
| 30 | 20 | -3.212 | -0.266 | 0.659 | 1.818 | 12.04 |
| 40 | 20 | -3.511 | -0.199 | 0.638 | 2.071 | 15.90 |
| 50 | 20 | -3.767 | -0.150 | 0.622 | 2.293 | 19.19 |
| 60 | 20 | -3.995 | -0.116 | 0.611 | 2.496 | 22.06 |
| 20 | 30 | -2.554 | -0.293 | 0.634 | 1.212 | 3.10 |
| 60 | 30 | -3.531 | -0.078 | 0.596 | 2.000 | 15.52 |
| 20 | 10 | -3.348 | -0.500 | 0.776 | 2.071 | 14.50 |
| 60 | 10 | -4.808 | -0.406 | 0.620 | 3.402 | 32.97 |

As an example, when $\sigma_h = 21.7$ MPa, $\sigma_H = 35.5$ MPa, $\sigma_V = 41.8$ MPa, and wellbore pressure $P = 35$ MPa, for notch geometry of $H = 20$ mm and $W = 20$ mm, the tensile stress at point A is

$$\sigma_x^A = -2.842 \times 21.7 - 0.355 \times 35.5 + 0.683 \times 41.8 + 1.513 \times 35 = 7.22(\text{MPa})$$

and at B is

$$\sigma_x^A = -2.842 \times 21.7 + 0.683 \times 35.5 - 0.355 \times 41.8 + 1.513 \times 35 = 0.68(\text{MPa})$$

The calculated stress values for other notch geometries under the same stress/pressure condition are summarized in the last column on Table 1. For all geometries assumed, the applied wellbore pressure 35 MPa is able to generate significant tensile stress around the notch. Deeper and narrower notch geometries tend to generate greater tensile stress. The results of an actual finite element simulation directly using these parameters are shown in *Figure 5(a)*. If we reduce the wellbore pressure to 27 MPa, three of the nine configurations will generate a tensile stress where the other six result in compression around the notch (results not shown but can be calculated quickly using the coefficients in Table 1).

Results for the fracture mechanics analysis are summarized in Table 2. Note that the T_x values in Table 2 are dimensionless whereas the K_x values in Table 2 has a unit of $\text{m}^{0.5}$.

Table 2. Coefficients for the transfer function of stress intensity factor near point A. The last column shows the stress intensity factor value corresponding to $\sigma_h = 21.7$ MPa, $\sigma_H = 35.5$ MPa, $\sigma_V = 41.8$ MPa, and $P = 35$ MPa.

| H (mm) | W (mm) | K_h | K_H | K_V | K_P | SIF^A (MPa) |
|----------|----------|---------|---------|--------|--------|---------------|
| 20 | 20 | -0.2384 | -0.0307 | 0.0527 | 0.2156 | 3.49 |
| 30 | 20 | -0.2688 | -0.0235 | 0.0496 | 0.2419 | 3.87 |
| 40 | 20 | -0.2935 | -0.0181 | 0.0469 | 0.2638 | 4.18 |
| 50 | 20 | -0.3148 | -0.0139 | 0.0448 | 0.2831 | 4.46 |
| 60 | 20 | -0.3338 | -0.0107 | 0.0431 | 0.3006 | 4.70 |
| 20 | 30 | -0.2292 | -0.0265 | 0.0527 | 0.2022 | 3.36 |
| 60 | 30 | -0.3168 | -0.0067 | 0.0469 | 0.2759 | 4.51 |
| 20 | 10 | -0.2461 | -0.0378 | 0.0519 | 0.2310 | 3.57 |
| 60 | 10 | -0.3490 | -0.0172 | 0.0365 | 0.3289 | 4.85 |

A concern of the EGS COLLAB team was that whether an axial fracture would develop and propagate before a transverse fracture can be initiated from the notch. The fluid pressure chosen for this analysis, namely 35 MPa, is lower than both σ_H and σ_V , which guarantees that no axial fracture can propagate under this pressure. As this pressure, can generate sufficient tensile stress for all the notch geometries examined, it proves that a transverse fracture will be generated from the notch before an axial fracture propagates from the wellbore. This conclusion applies even if

there already exists an axial fracture or a fracture that intersects the wellbore and is sub-parallel to the wellbore.

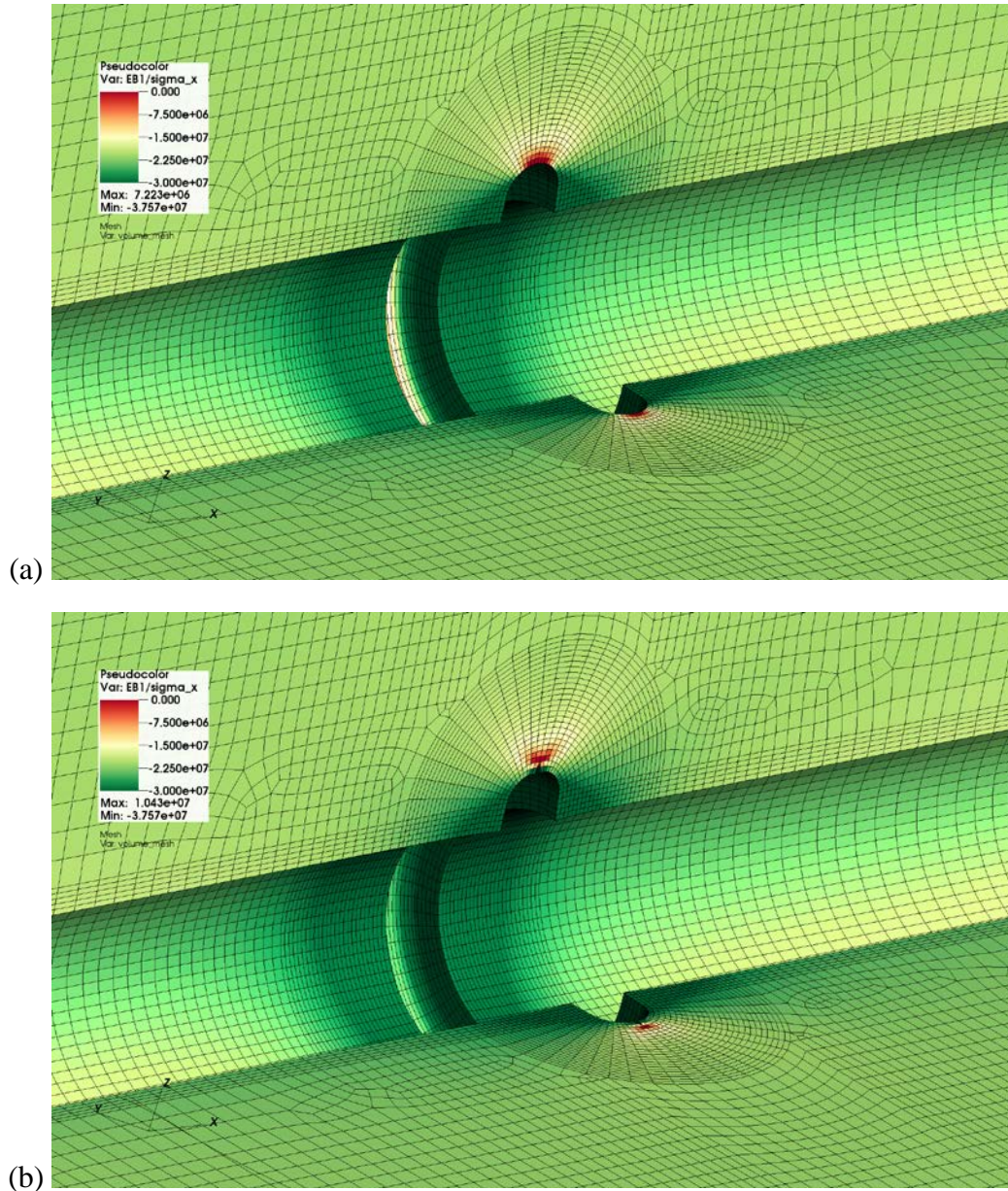


Figure 5: σ_x in the rock around the wellbore and the notch assuming $\sigma_h = 21$ MPa, $\sigma_H = 40$ MPa, $\sigma_V = 42$ MPa, and wellbore pressure $P = 35$ MPa for (a) smooth notch surface and (b) notch with a 4-mm deep crack around the notch. Deformation is magnified by 300 times.

5. Circulation Experiments without Fracture Growth

To design the circulation experiments, particularly to make equipment procurement plans and calculate circulation durations, it is necessary to have an estimate of the expected circulation rate.

It is desired to have a relatively high circulation rate to be able to observe thermal breakthrough within a reasonable experiment time. A constraint is that injection pressure during circulation tests should not be high enough to propagate the fracture. The LLNL team estimated achievable circulation rates for two scenarios: 1) assuming homogeneous in situ stress distribution and an idealized penny-shaped fracture, and 2) assuming a heterogeneous stress field and a somewhat irregular fracture shape.

In the homogeneous stress scenario, we first simulate the hydraulic fracturing process using LLNL's GEOS code (Settgast et al. 2017; Fu et al., 2013) assuming a normal in situ stress of 20 MPa, an injection rate of 0.1 L/s, an injection duration of 10 minutes, and a rock toughness of 1.0 MPa(m)^{0.5}. This resulted in a penny-shaped fracture 15 m in radius. A shut-in simulation showed minimal post shut-in growth and a residual net pressure of 200 kPa in equilibrium with the toughness.

For simulating circulation, we apply a static fluid pressure of 20.2 MPa at the injection well while slowly decreasing the pressure at the production well (10 m from injection well) from 20.2 MPa to zero. We observe the flow rate into the production well as a function of the back-pressure applied at the production well. During the entirety of the process, the fluid pressure across the whole fracture is below 20.2 MPa and it is not sufficient to overcome the rock toughness to continue to propagate the fracture. Therefore, the fracture geometry remains static. The mesh resolution is 0.4 m and the model includes more than 1.6 million elements.

As the production, back-pressure decreases, two competing mechanisms affect the production flow rate. First, the inter-well pressure-drop increases, which tends to increase flow rate. Second, the fracture aperture around the production well decreases as the pressure decreases (i.e. choking), which tends to impede flow.

This simulation also requires a constitutive relationship for the aperture of mechanically closed fracture (two walls in contact) as a function of the effective stress. We use the widely accepted Barton-Bandis model. Considering that the maximum aperture achieved during the stimulation was 163 microns, we assume the fracture aperture at zero-effective stress is 40 microns and the aperture reduces to 20 microns at an effective stress of 5 MPa. Fracture aperture under the closed condition is affected by the surface asperity of the fracture and cannot be predicted *a priori*. A snapshot of the fluid pressure and fracture aperture distributions when the back-pressure is at 19.15 MPa is shown in Figure 6.

The production well flow rate as a function of back-pressure applied at the production well is shown in Figure 7. The highest flow rate is achieved when the back-pressure is slightly lower than σ_h . Further reduction of the back-pressure causes greater near-wellbore choking of the flow. The highest flow rate is 0.065 L/s, in the same order of magnitude as the kISMET stimulation injection flow rate. For the case with heterogeneous stress, we first stochastically generated a normal stress field that has 1) a mean value of 20 MPa at the injection depth, 2) an average vertical gradient of 14 kPa/m, and 3) a zero-mean perturbation with a standard deviation of 0.5 MPa and an auto-correlation length of 5 m, generated using the method documented in Guo et al. (2016). The stress distribution and the fracture shape predicted using GEOS after 10 mins of 0.1L/s injection are shown in Figure 8(a).

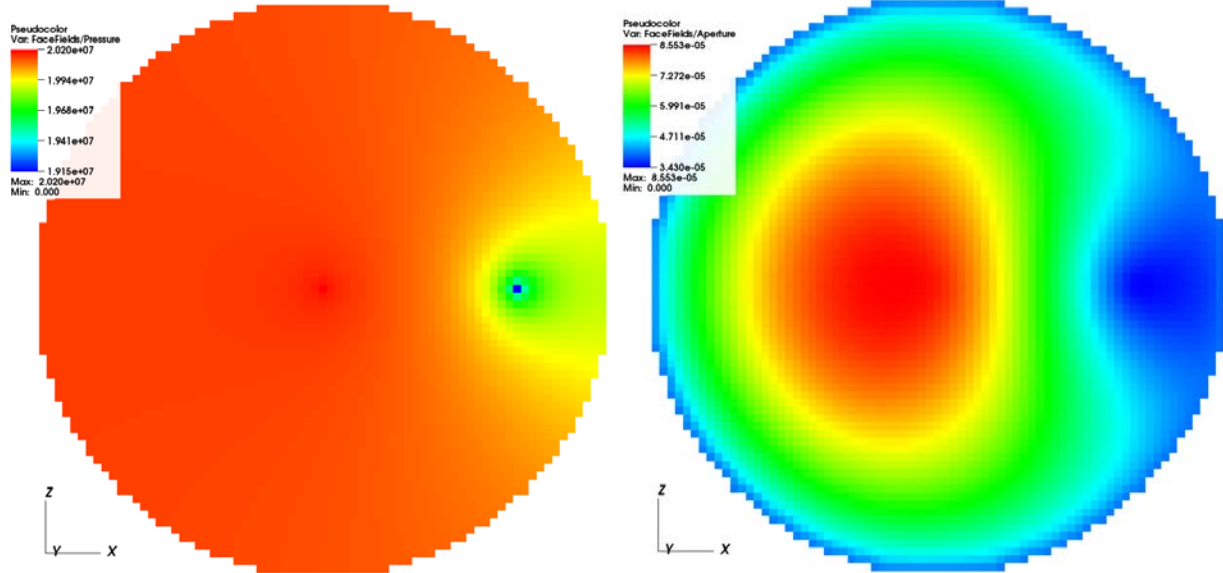


Figure 6: The fluid pressure (left) and aperture (right) distributions on the penny-shaped fracture.

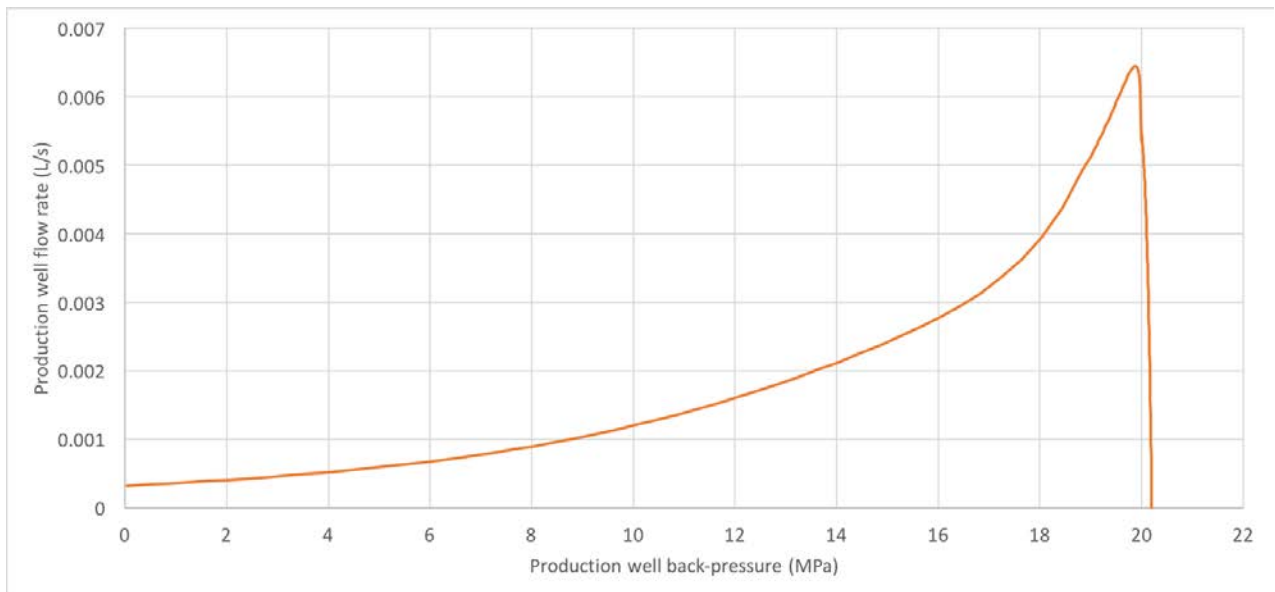


Figure 7: Production well flow rate as a function of back-pressure applied at the production well. The pressure at the injection well is kept constant at 20.2 MPa, a value ensures that the fracture will not propagate.

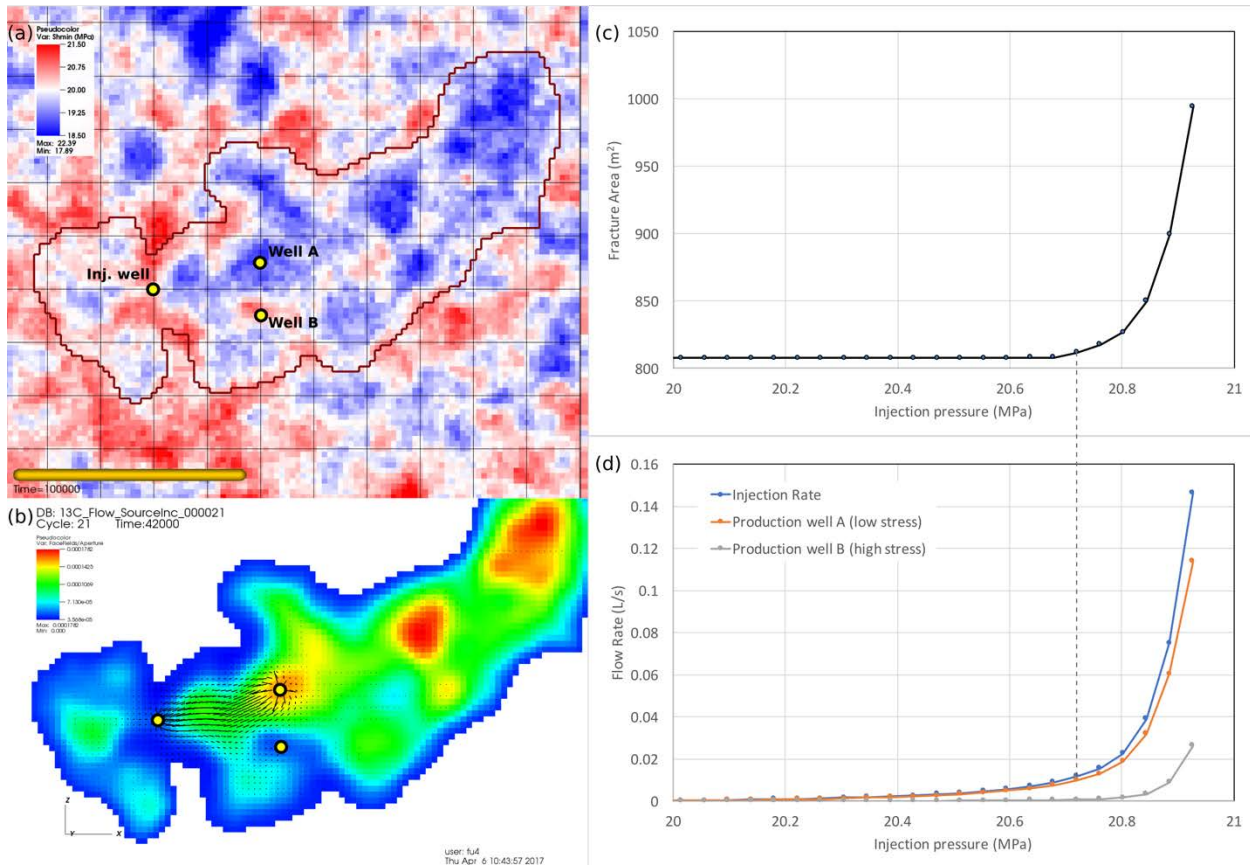


Figure 8: Simulation to estimate circulation rate along the fracture generated under heterogeneous stress with a standard deviation of 0.5 MPa. (a) The well layout in relation to the stress field. (b) The aperture and flow fields when the injection pressure reaches 20.68 MPa. (c) The fracture area as a function of the injection pressure. The fracture propagation resumes when the injection pressure is above 20.7 MPa. (d) The flow rates through the three wells as a function of the injection pressure.

The circulation pressure control strategy that we have used to evaluate the circulation rate for the ideal penny-shaped fracture, namely fixing the injection pressure at the shut-in pressure while varying the back-pressure from the production well, does not apply to the fractures under heterogeneous stress fields. This is because for the latter scenarios, the final shut-in pressure is controlled by the lowest “stress pocket” that the fracture encounters and in the final shut-in state most area of the fracture has closed. For the heterogeneous stress field the method is to hold the back-pressure in the production well(s) at the final shut-in level while gradually increasing the injection pressure until the fracture starts to significantly grow again.

We place two production wells, well A at a low stress region and well B at a high stress region as shown in Figure 8, each of which is 10.3 m from the injection well. As the injection pressure gradually increases, the fracture near well A is expected to open when that near well B remains closed. The simulation results in Figure 8 (b) through (d) show that the fracture starts to grow again when the injection pressure reaches 20.7 MPa, when the combined production rate is

0.0083 L/s, of which more than 90% is contributed by well A which intersects the fracture at a low stress region.

The simulations for both scenarios show that the maximum achievable circulation rate without continuing to propagate the fracture is likely below 0.01 L/s. When spatial variation of stress is significant, there exists the risk of production wellbore encountering the fracture at a high stress region and the circulation rate might be one order of magnitude lower than the maximum value.

6. Conclusions

The extreme temperature and depth environments of enhanced geothermal systems (EGS) make experimental investigations challenging and costly as proven by the hot-dry rock experiments at Fenton Hill, New Mexico, USA. The United States Department of Energy, Geothermal Technologies Office (GTO) seeks to establish a new field-scale EGS research facility, the Frontier Observatory for Research in Geothermal Energy (FORGE), and currently is in the set-up and characterization stage of selecting a site. In the interim GTO is supporting a collaborative study that will serve as a research and development bridge between the more conventional laboratory-scale stimulation and rock mechanics experiments and the field-scale studies envisioned for FORGE. This collaborative study, called EGS Collab, is being led by the Lawrence Berkeley National Laboratory (LBNL) and involves other national laboratories, universities and private industry teaming to conduct stimulation and circulation experiments, and verify computer codes, numerical algorithms and approaches, and process models against the generated data. This three-year project has been tasked with providing new knowledge and modeling capabilities, forming a bridge from laboratory scale to the field scale of FORGE.

Numerical simulation is an essential component of the EGS Collab project in two respects. First numerical simulation is contributing to the design of the meso-scale experiments that will be conducted under *in-situ* stress conditions and crystalline rock formations. Second the experimental measurements will serve as benchmarks against which to compare post-experimental numerical simulations. Heterogeneities in the rock fabric, natural fractures, spatial variations of *in-situ* stress, and other geologic features generally preclude numerical simulation from providing accurate matches to experimental outcomes. The true value of numerical simulation then comes from the understanding it provides concerning complex system behavior, allowing scientists and engineers to make informed choices about experimental designs and interpreting experimental observations. This paper was specifically concerned with addressing five questions associated with the EGS Collab experiments.

The *in-situ* stress conditions at the first experimental site indicate the formation of a vertical fracture under hydraulic stress conditions. As the West Access Drift at the 4850 Level, will allow for drilling in vertical and horizontal orientations, an early question for the EGS Collab experiment was the orientation of the boreholes. To address this question a series of numerical simulations were executed by teams from The University of Oklahoma and Idaho National Laboratory that modeled fracture initiation and propagation from different stimulation borehole orientations, with respect to the principal stress directions and magnitudes. Whereas the preferred orientation for the boreholes in terms developing circulation patterns within the generated fracture was horizontal or near horizontal, the outcomes from the simulations indicated that fracturing would initiate in an axial direction and then rotating transverse to the borehole in response to minimum principal stress. These simulations indicated that if horizontal or near

horizontal boreholes were to be chosen, notching of the borehole would be required to generate fractures initially oriented transverse to the borehole.

To address the question concerning seismic events during stimulation a coupled flow and quasi-state discrete element method (DEM) model was executed by Idaho National Laboratory to provide estimates of the seismic events, initial breakdown pressure, propagation pressure, and fracture geometry. Without an *in-situ* stress gradient included into the model, the simulated hydraulic fracture is similar to the penny shape crack expected for tensile hydraulic fracturing in an infinite homogeneous material. Due to the presence of local-scale mechanical heterogeneity incorporated into the DEM model, it is quite interesting to observe the random ‘pinning’ and ‘depinning’ of the propagating fracture front in the simulations. In addition, the pre-test simulation provides an initial estimate of the magnitude of induced seismic events related to hydraulic fracturing at the EGS Collab site. The majority of the events are very low-magnitude events, too small to be any concern in terms of induced seismic hazard).

The final experimental design element addressed via numerical simulation approaches and tools was the circulation experiments and how to execute those experiments without incurring additional growth of the fracture. For this analysis the Lawrence Livermore National Laboratory executed numerical simulations for two scenarios: 1) assuming homogeneous *in situ* stress distribution and an idealized penny-shaped fracture, and 2) assuming a heterogeneous stress field and a somewhat irregular fracture shape. The simulations for both scenarios show that the maximum achievable circulation rate without continuing to propagate the fracture is likely below 0.01 L/s. When spatial variation of stress is significant, there exists the risk of production wellbore encountering the fracture at a high stress region and the circulation rate might be one order of magnitude lower than the maximum value.

REFERENCES

- Barton, N., Bandis, S., Bakhtar, K., 1986. Strength, deformation and conductivity coupling of rock joints. *Int. J. Rock Mech. Min. Sci.* 22 (3), 121–140.
- Duchane, D.V., and W.W. Winchester. 1993. *Hot Dry Rock Energy Annual Report Fiscal Year 1992*, Los Alamos National Laboratory, LA-UR-93-1678, Los Alamos, New Mexico, USA.
- Gaston, D, L Guo, G Hansen, H Huang, R Johnson, H Park, R Podgorney, M Tonks, and R Williamson. 2012a. "Parallel Algorithms and Software for Nuclear, Energy, and Environmental Applications Part I: Multiphysics Algorithms," *Communications in Computational Physics (Print)*, 12(3):807-833.
- Gaston, D, L Guo, G Hansen, H Huang, R Johnson, H Park, R Podgorney, M Tonks, and R Williamson. 2012b. "Parallel Algorithms and Software for Nuclear, Energy, and Environmental Applications Part II: Multiphysics Software," *Communications in Computational Physics (Print)*, 12(3):834-865.
- Oldenburg, C.M., P.F. Dobson, Y. Wu, P.J. Cook, T.J. Kneafsey, S. Nakagawa, C. Ulrich, D.L. Siler, Y. Guglielmi, J. Ajo-Franklin, J. Rutqvist, T.M. Daley, J.T. Birkholzer, H. Wang, N.E. Lord, B.C. Haimson, H. Sone, P. Vigilante, W.M. Roggenthen, T.W. Doe, M.Y. Lee, M. Ingraham, H. Huang, E.D. Mattson, J. Zhou, T.J. Johnson, M.D. Zoback, J.P. Morris, J.A. White, P.A. Johnson, D. DD. Coblentz, and J. Heise. 2016. *Intermediate-Scale Hydraulic*

- Fracturing in a Deep Mine, kISMET Project Summary 2016*, Lawrence Berkeley National Laboratory, LBNL-1006444.
- Podgorney, RK, H Huang, and D Gaston. 2010. A Fully-Coupled, Implicit, Finite Element Model for Simultaneously Solving Multiphase Fluid Flow, Heat Transport, and Rock Deformation. *Proceedings: Geothermal Resources Council Annual Meeting*, Sacramento, CA.
- U.S. Department of Energy, Energy Efficiency & Renewable Energy, Geothermal Technologies Office. 2017. *2016 Annual Report Geothermal Technologies Office*, Retrieved from https://energy.gov/sites/prod/files/2017/03/f34/GTO%202016%20Annual%20Report_0.pdf.
- Zyvoloski, A. G. 2007. *FEHM: A control volume finite element code for simulating subsurface multi-phase multi-fluid heat and mass transfer*. Los Alamos Unclassified Report LA-UR-07-3359.
- White, M.D., P. Fu, and M.W. McClure. 2017. “Outcomes from a collaborative approach to a code comparison study for enhanced geothermal systems.” *Proceedings: 42nd Workshop on Geothermal Reservoir Engineering*, Stanford University, Stanford, CA, USA.
- White, M.D., McClure, M.W., Fu, P., Cheng, Q., Elsworth, D., Gan, Q., Hao, Y., Im, K.J., Safari, R., Tao, Q., Xia, Y., Podgorney, R.K., Danko, G., Bahrami, D., Chiu, K., Fang, Y., Gao, Q., Horne, R.N., Norbeck, J., Sesetty, V., White, S.K., Kelkar, S., Ghassemi, A., Barbier, C., Detournay, C., Furtney, J.K., Guo, B., Huang, K., Rutqvist, J., Sonnenthal, E., Wong, Z. 2016. *Benchmark Problems of the Geothermal Technologies Office Code Comparison Study*, Pacific Northwest National Laboratory, PNNL-26016.
- Zhou, J., H. Huang, E. Mattson, H.F. Wang, B.C. Haimson, T.W. Doe, C. Oldenburg, and P.F. Dobson. 2017. “Modeling of hydraulic fracture propagation at the kISMET site using a fully coupled 3D network-flow and quasi-static discrete element model.” *Proceedings: 42nd Workshop on Geothermal Reservoir Engineering*, Stanford University, Stanford, CA, USA.
- Guo, B., Fu, P., Hao, Y., and Carrigan, C.R. (2016). “Thermal drawdown-induced flow channeling in a single fracture in EGS”. *Geothermics*, 61:46-62.
- Settgast, R.R, Fu, P., Walsh, S.D.C, White, J.A., Annavarapu, C., and Ryerson, F.J. (2017). “A Fully Coupled Method for Massively Parallel Simulation of Hydraulically Driven Fractures in 3-Dimensions”. *International Journal for Numerical and Analytical Methods in Geomechanics*, 41(5): 627-653).
- Fu, P., Johnson, S.M., and Carrigan, C.R. (2013). “An explicitly coupled hydro-geomechanical model for simulating hydraulic fracturing in complex discrete fracture networks.” *International Journal for Numerical and Analytical Methods in Geomechanics*, 34(14): 2278-2300.